Multiplex detection of cell surface markers using Surface Plasmon Resonance Imaging

Carolina de Freitas Pereira Ruivo
Under the supervision of Professor Luis Fonseca[1]* and Ivan Stojanovic [2]*

Abstract
Surface Plasmon Resonance (SPR) is an established technique for detection of molecular binding. More recently, new experimental set ups transformed SPR in a label-free and real-time detector of specific cell binding to an immobilized ligand.
In this work, Surface Plasmon Resonance Imaging (SPRi) was employed to investigate the feasibility of a multiplex sensor to detect simultaneously 44 different cell surface antigens. For this purpose, a total of 5 cancer cell lines KG1a, MCF7, MG-63, NCI-H460 and SK-BR-3 and peripheral blood cells from healthy donors were used to illustrate the potential of this sensor.
For cancer cells, SPR curves showed a variety of responses to each one of the targeted antigens, proving the ability of this sensor to characterize multiple cell surface molecules. Regarding the peripheral blood cell measurements, frequent leukocytes populations such as T-cells and Granulocytes were easily identified. Furthermore, measurements performed on samples spiked with cancer cells showed that based on specific cancer antigens response, cancer detection in a complex sample is possible.
Exploring the factors behind the detected SPR signals, a comparison with flow cytometry showed a relation between the response intensity and the number of antigens on the cell surface. A study of the number of cells binding to the sensor and the cell area effect on the signal also demonstrated a proportional relation with intensity. Also, single-cell image based analysis indicated that individual cell binding can be monitored by reflectivity variation.
In conclusion, here it was illustrated that SPRi allows the simultaneous observation of cell binding to multiple markers and suggests that antigen quantification can be achieved.

Keywords
Surface Plasmon Resonance — Multiplex sensor — Cell surface biomarkers — Flow Cytometry — Cancer cell lines — Cell-antibody interaction

[1] *Department of Bioengineering, Instituto Superior Técnico*
[2] *Medical Cell Biophysics Group, MIRA Institute, University of Twente*

1. Introduction

1.1 Surface Plasmon Resonance

The electrons part of the conduction band of noble metals, such as gold, can undergo a collective oscillation when excited by an oscillating electromagnetic field like light [1]. These oscillating electrons, corresponding to a propagating electronic density wave, are called plasmons. At a specific light wavelength, the resonance of the plasmons causes the exciting light extinction.

Surface plasmons (SP), occurring on the interface between a metal and a dieletric, have their resonance highly dependent on the media dielectric constant and therefore on the refractive index [2]. For the resonance to occur, a specific light, with a certain wavevector, must induce a polarization of the electrons of the metal conduction band and enter resonance with the plasmons [3].

Both structures, metal and dielectric metal, dimensions influence the optical properties of plasmons. In case of structures with dimensions superior to light wavelength, like the case of thin metallic films, plasmons cannot be directly excited [5]. To achieve the resonance frequency, the light wavevector must be incremented such a way that light frequency equals *ksp*, see **Equation 2**.

For the SP excitation to occur light must be p-polarized, such that its electric field oscillates in the z-direction. The resulting SP will also oscillate in the z-direction, as can be seen in **Figure 1**.

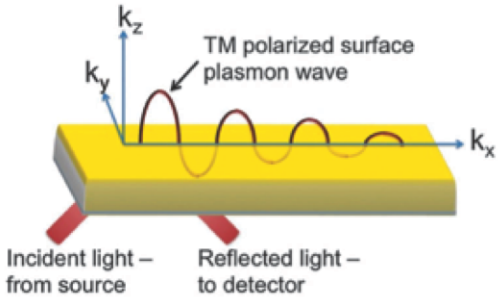

Figure 1. Excitation of surface plasmons with a prism coupling configuration. Extracted from [5].

The exciting light frequency *Kx* can be given by original frequency *Ko*, incident angle θ, and the dielectric constant η_D, **Equation 1**:

$$K_x = K_o \eta_D \sin(\theta) = \frac{2\pi}{\lambda} \eta_D \sin(\theta) \tag{1}$$

Hence, for an equal plasmon frequency **Equation 2** is obtained:

$$K_x = K_{sp}; \frac{2\pi}{\lambda} \eta_D \sin(\theta) = \frac{\omega}{c} \sqrt{\frac{\varepsilon_m(\lambda)\varepsilon_s(\lambda)}{\varepsilon_m(\lambda) + \varepsilon_s(\lambda)}} \tag{2}$$

According to these equations, the light wavevector can be modulated by changing the light wavelength or angle of the incidence beam. The light frequency modulation by incident angle is called scanning angle configuration, and the wavelength modulation is known as wavelength-modulated SPR [5]. The commercial SPR instrument used in this work has a scanning angle configuration.

1.2 Surface Plasmon Resonance biosensing

As mentioned previously a thin metal layer can be used as a plasmon source material. The SP generated will be sensitive to the dielectric constant of a thin layer in contact with the metal. Therefore, a change in the refractive index (thus dielectric constant) due to bulk or biding events, will lead to a consequent change in SP wavelength or the light beam angle. A limitation to a direct application of the SP resonance, is that any type of change on the evanescent field will be sensed without any specificity. For biosensing purposes, efforts have been made to improve a surface chemistry capable of immobilizing a molecular receptor and an analyte-specific molecular receptor such as an antibody.

When an analyte is captured by its respective molecular receptor, it will cause a small but detectable change of the local refractive index hence, a change in the SPR signal. The change in the SPR signal is translated to an angle shift of the SPR dip.

The SPR dip corresponds to the angle of resonance where light is resonating with plasmons and therefore it is not reflected back to the detector. The angle or SPR dip plotted as a function of time is called a sensorgram, see **Figure 2**. Typically, the angle shift overtime is represented in resonance units (RU). One RU corresponds to an angle shift of 0.1 m°.

Classical SPR biosensing is used for biomolecules such as proteins. The RU response gives an indication of the amount of molecules bound to the surface compared with the baseline.

1.3 Cell detection using SPR

In recent years, cell detection has been gradually explored, showing promising results and applications. The SPR principle, previously explained for the detection of analytes in the close surroundings of a sensing metal layer, is now applied to detect a small part of the cell surface, correspondent to the evanescent field (approximately 300nm much smaller than cell height) that interacts with the immobilized ligand.

Despite the small sensing depth, many valuable cellular studies can be performed, including physiological changes, interaction with the surface and response to the ligand. Also, variety of cells such as bacteria, mammalian cells and virus have been reported [7].

The great majority of the available studies, explored cell detection based on specific molecular receptors that recognize a specific molecule on the cell plasma membrane [8], [9], [10] among others. However, some studies where the goal was to investigate differences on cell response caused by external stimuli, described cell growth on the top of the sensor previous to the measurement, without the use of any specific marker [11] and [12].

1.4 Cell surface molecules as biomarkers

NIH defines a biomarker as a characteristic that is objectively measured and evaluated as an indicator of normal biological processes, pathogenic processes, or pharmacologic responses to therapeutic.

In this sense, cell surface molecules that can be

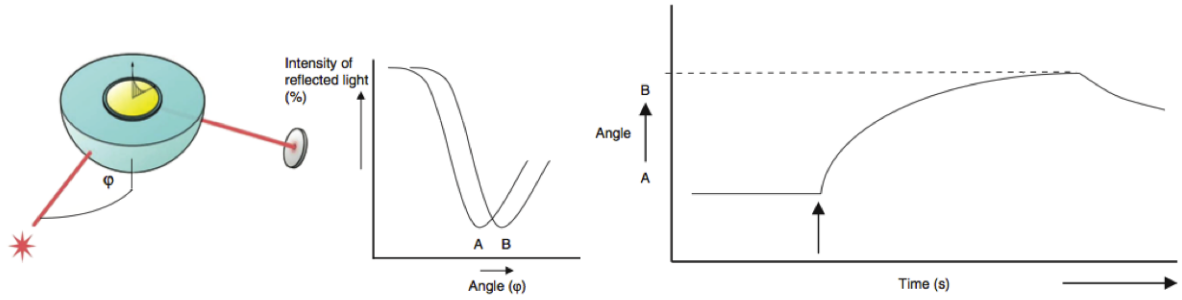

Figure 2. Schematic experimental set-up of surface plasmon resonance excitation and its representation over time. On the left: a sensor with a gold coating is placed on a hemisphere (or prism). Reflected light intensity is measured in the detector (disk). At a certain angle of incidence (j), excitation of surface plasmons occurs, resulting in a dip in the intensity of the reflected light. On the right: The change in refractive index will cause an angle shift from A to B that is plotted over time in a sensogram.Extracted from [4].

detected and quantified are considered biomarkers for both cell differentiation and pathology indicators.

The multiplex sensor developed in this work had the objective of detecting firstly, cancer cells, and secondly peripheral blood cells, using cell surface molecules as biomarkers to characterize and distinguish both cell types.

Cell surface antigens that are overexpressed, mutated or selectively expressed compared with normal tissues are considered as potential biomarkers.

Based on literature reported cancer and blood relevant biomarkers, a total of 44 antigens were selected as targets for the intended sensor in this study. The selected antigens were divided into cell origin, drug targets and cell adhesion markers, see **Tables 1 2 and 3**.

Table 1. Cell Origin markers for blood and cancer cells.

Cell Origin markers		
Marker	**Expression**	**References**
CD3	T lineage cells	[19] [20]
CD8a	T lineage cells	[19] [21]
CD11c	Dendritic cells	[19] [22]
CD14	Monocytes and osteoclast progenitors	[19] [23]
CD19	B cells	[19] [24]
	Malignant B cells	[25]
CD20	Mature B cells	[19] [26]
CD25	Regulatory T-cells	[19] [27]
CD33	Myeloid lineage Overexpression on monocytes and macrophages	[19] [28]
CD45	All leukocytes	[19]
CD56	NK cells Neuro cells Embryonic tissue and tumors	[19]
CD61	Platelets and megakaryocytes	[19]
CD66b	Granulocytes	[19] [29]
CD105	Vascular endothelial cells Mesenchymal cells Intra-tumor expression	[19] [30]
CD123	Committed hematopoietic progenitor cells Dendritic cells	[31]
CD140a	Megakaryocytes Myeloid precursors	[19]
CD146	Endothelial cells Endothelial cells Some epithelium Melanoma cells	[19]
CD235a	Erythrocytes	[19]
CD326	Epithelial cells Tumors	[19] [32]

2. Materials and Methods

Cells

For the conducted SPR measurements, cells from 5 different cell lines were selected: KG1a (ATCC®CCL246.1™) derived from bone marrow presenting acute myelogenous leukemia, MCF7(ATCC®HTB-22™) derived from mammary gland adenocarcinoma, MG-63(ATCC®CRL-1427™) derived from osteosarcoma, NCI-H460(ATCC®HTB-177™) derived from large cell lung carcinoma, and SK-BR-3(ATCC®HTB-30™) derived from mammary gland adenocarcinoma.

For cell harvesting and subculture purposes, 0.05% Trypsin-0.02% EDTA (Sigma-Aldrich®) was used to loosen adherent cells from the flask bottom wall.

Blood Samples

Blood samples, from anonymous healthy donors, used in this work were provided by the ECTM donor service, part of the MIRA institute (Twente University). Blood samples were drawn shortly before the performed measurements. To facilitate peripheral blood cells detection on SPR, the blood samples were lysed.

SPRi

The Continous Flow Microspotter (CFM) (Wasatch microfluidics LLC®) was used for ligand spotting on the sensor surface. In this work only unlabeled antibodies were used as ligands. Different spot densities were obtained by dilution of commercial antibody solutions in the immobilization buffer (1.93 parts of sodium acetate

Table 2. Drug Targets markers for blood and cancer cells.

Marker	Expression	References
Drug target markers		
CD71	Acute myeloid leukemia Breast carcinomas	[33] [34] [35]
CD117	Overexpressed in small-cell lung carcinoma and Gastric cancer	[36] [37]
CD221	Overexpressed in Multiple myeloma Glioma, Breast, Prostate, Pancreas and Thyroid cancer	[38] [39] [19]
CD227	Overexpressed in Breast, Colon, Lung and Ovarian cancers	[40] [41] [42]
CD261	Colon, Lung and Pancreas tumors 2* Hematological malignancies	[43] [19]
CD262	Colon, Lung and Pancreas tumors 2* Hematological malignancies	[44] [19]
CD309	Angiogenesis regulation	[45] [46] [19]
EGFR	Overexpressed in Glioma, Lung, Breast, Colon and Head/Neck tumors	[47] [48] [49] [50] [19]
HER2	Overexpressed in Breast, Colon, Ovarian and Prostate cancer	[51] [52] [19]
HER3	Overexpressed in Breast, Colon, Ovarian and Prostate cancer	[53] [19]

Table 3. Cell adhesion markers for blood and cancer cells.

Marker	Expression	References
Cell adhesion markers		
CD24	B lineage cells Overexpressed in pancreatic, ovarian, breast, prostate, small cell lung and CSC	[54] [55] [56]
CD44	Leukocytes and erythrocytes Gastric, Colon, CSC and breast cancers	[56] [57] [58] [59]
CD49a	Activated T-cells Monocytes and NK cells Fibroblasts, Hepatocytes and melanoma	[60] [19]
CD49b	Platelets and T-cells Overexpressed in colon and breast cancer	[61] [19]
CD49c	T and B cellsAdherent cell lines Overexpressed in pancreatic cancer	[62] [19]
CD49d	T and B cells Monocytes Colon cancer	[63] [19]
CD49e	T and B cells Osteoblasts and endothelia	[64]
CD49f	Platelets, Monocytes and T cells Adherent cell lines Colorectal and prostate cancer	[65] [66] [19]
CD103	Lymphocytes and T-cells Overexpressed in lymphomas	[67] [19]
CD104	Cells on the basal layer of epithelia Overexpressed in squamous cell carcinoma, thyroid, colon, gastric and pancreatic carcinomas.	[68] [19]
CD106	Endothelial cells Colorectal cancer	[69] [19]
CD113	Epithelial cells Overexpressed in Breast cancer	[19]
CD144	Endothelial cells Overexpressed in melanomas	[19]
CD166	CSC Overexpressed in Colon and Breast cancer	[19]
CD324	Overexpressed in Breast and Gastric Carcinomas	[19]

and 3.07 parts of acetic acid).

The SPR gold layer sensors used in all the conducted SPR measurements were the Easy2spot^{TM}pre-activated G-type sensor (Ssens®). This sensor has a modified surface chemistry containing active ester groups that allow a covalent biding of the ligants.

Before SPR cell measurement, it was necessary to deactivate the sensor in order to avoid unspecific adherent behavior. Sensor deactivation was achieved injecting two buffers separately, 1% Bovine Serum Albumin (BSA) solution in ligand immobilization buffer and 100mM 2-aminoethanol solution with a pH of 8 [13].

The SPR platform used for the measurements presented in this work, is the IBIS MX96 (IBIS Technologies®). The regions-of-interest ROIs, which represent the areas where the shift of the resonance angle is determined, can be placed manually on top of the printed spots. In addition, ROIs used as references can be placed next to the spot of interest and subtracted in post-measurement analysis, in a process called local referencing.

Flow cytometry

Flow cytometry is the established gold-standard technique used to analyze cell surface antigens, with the advantage of providing a reliable and precise antigen quantification.To validate the results obtained with the SPR cell measurements, antigen quantification was obtained using BD FACS Aria II®flow cytometer. Fluorescent immunostaining was achieved using an anti-IgG PE (Abcam®).

Additionally to the fluorescent labeled cells measurements, QuantiBRITE PE beads (BD®) were also used to quantify the number of antigens bound per cell (ABC).

3. Results and Discussion

3.1 Cell response measurement conditions

Cell response to spot density

The primary objective was to identify the effect of the antibody spot density on cell response, using multiple markers and various cell lines. This would allow the selection of an optimal concentration of the antibody solution to use in subsequent measurements. For this purpose, antibodies solutions were prepared with immobilization buffer (pH 4.45) in serial dilutions (1:2) starting from 10 down to 0.08µg/mL.

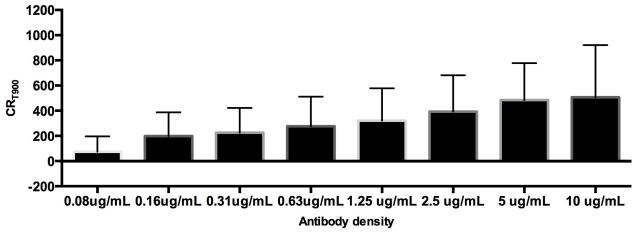

Figure 3. Analysis of CRT_{900} values obtained from the sensorgrams of the cell response associated with the tested spot densities. Filled bars in the graph correspond to the average CRT_{900} value and the small bars to the data standard deviation.

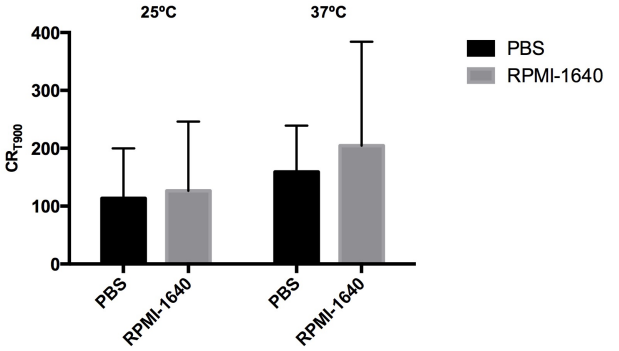

Figure 4. Analysis of CRT_{900} values of the cell response associated with temperature and buffers. Filled bars in the graph correspond to the average CRT_{900} value and the small bars to the data standard deviation.

To find an actual quantifiable difference between the various spot concentrations and their cell response (RU) at 900s of association time (CRT_{900}) values were taken into account and an average was obtained for each tested density **Figure 3**. Concerning denser spots, it is noticeable that for antibody densities of 10µg/mL and 5µg/mL the average response is actually similar (average difference is less than 4 percentage points). To lower densities there is a constant decrease of the average response up until the lowest density of 0.08µg/mL, which is practically indistinguishable from the signal obtained from the sensor background.

Considering this cell response analysis, 5µg/mL was the spot density used for further measurements, preventing excessive use of antibodies and allowing to obtain a cell response quite close to the maximal response typical from a denser spot.

Cell response to temperature and measurement buffer

The secondary objective of this SPR analysis study, was to investigate the influence of measurement conditions, namely temperature and buffer solution used to resuspend the cell sample.

In order to evaluate the effect of these conditions on a SPR measurement four different scenarios were tested, combining two possible temperatures: 37 and 25 °C (approximately room temperature), and two suitable buffers for short period measurements: PBS and complete culture medium RPMI-1640 (Sigma-Aldrich®).

Once again, for the sake of quantitative comparison, the values of CRT_{900} were taken into account and their average was plotted in **Figure 4**. It is clear that the cell response is higher for a measurement at 37°C when compared to 25 °C independently of the buffer.

For the further presented measurements, the temperature was settled at 37°C and both buffers were used depending no the sample to be tested: culture medium for cancer cell lines and PBS for peripheral blood cells.

Figure 5. Multiplex sensor scheme example used for SPR measurements. From the available 48 spots, 44 were used for the selected biomarkers and 4 as spot controls. CFM spotter was used to print the antibodies with a density of 5µg/mL on a G-type sensor.

3.2 SPR analysis

After defining the SPR measurement parameters that positively affect the cell response, a sensor was designed with 44 biomarkers relevant for cancer cells and peripheral blood cells. The final goal of this project was to investigate the feasibility of a multiplex platform developed in a commercially available SPRi technology, a total of five cell lines and a small number of peripheral blood samples where tested in the designed sensor.

Cancer cell lines

The multiplex concept has already been explored in the SPR field applied to protein ligands. Regarding cell measurements, up to this date few studies have communicated to use a considerable number of different markers. Here the possibility of measuring simultaneously, in a real-time and label-free manner, the cell biding to 44 different antibodies targeting relevant antigens present on the surface of cancer cells was investigated. The sensorgrams on **Figure 6** show that cancer cell detection can be achieved by characterization of multiple surface antigens. For the five studied cell lines is possible to

find unique responses for several available biomarkers on the designed sensor. Flow cytometry, as referred, is currently the gold-standard technique used to examine cell surface antigens. Typical flow cytometry instruments have about 12-colours systems but up to 17 different colors plus two physical parameters have been described [70]. Multiparameter cytometry was also used to isolate malignant plasma cells in multiple myeloma [71]. However, the configuration of this type of measurement is quite complex, a precise system calibration and an optimal fluorescent resolution are necessary to avoid channel cross-talk that can affect a correct detection[72]. Roughly comparing, a multiplex SPR analysis seems to overcome the complexity of such cytometry multiparametric measurement, allowing to detect a clear signal for each of the markers without the necessity of a multiple-label staining protocol or calibration. Regardless, the study of SPR cell detection is in a too early stage to be considered as an alternative to flow cytometry, since no precise antigen quantification is not yet possible.

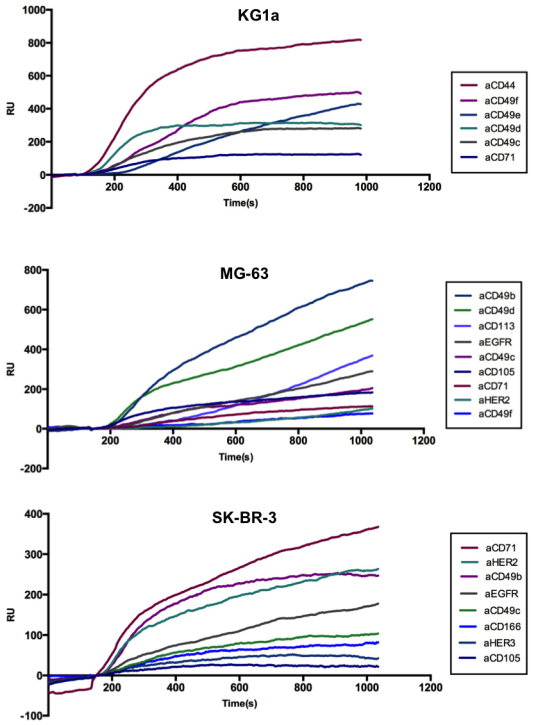

Figure 6. Sensograms obtained with the multiplex sensor for KG1a, MG-63 and SK-BR-3 cells with a concentration of 1 million cells/mL.

Peripheral blood cells

It is possible to detect peripheral blood cells binding specifically to the designed SPR sensor as it as been demonstrated by the label free detection of erythrocytes [73]. Highly frequent cells, such as T-cells and Granulocytes, can easily be identified in the sensorgrams and visualized in the sensor images, see **Figure 7**. Using specific antibodies to certain cell sub-types creates the opportunity to discriminate sub-populations on these cells. For less frequent and more complex antigen characterization cells such as B-cells and NK-cells, SPR analysis does not seem to be not conclusive. The impossibility of measuring multiple markers simultaneously for the same cell, does not allow to conclude about the presence of those cells types in the blood sample.

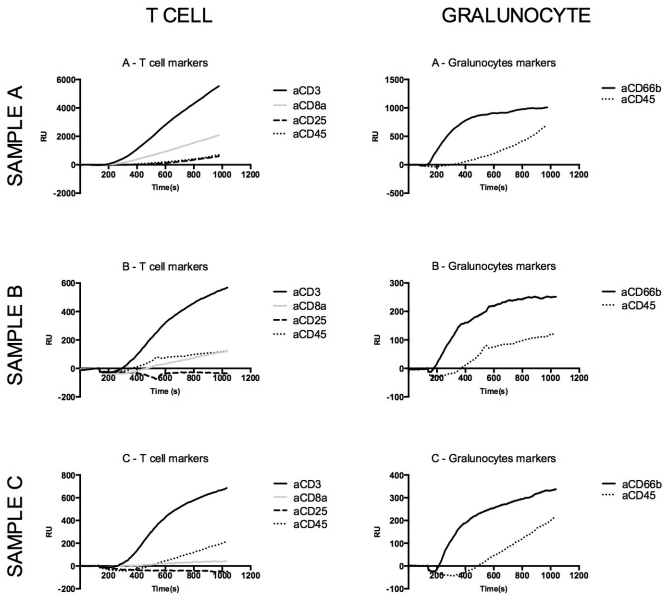

Figure 7. Sensorgrams from the 3 different blood samples (A,B and C) for specific T-cells and Granulocytes markers. The cell sample was obtained by erythrocytes lysis.

Spiked blood

Taking the advantage of a multiple marker measurement, cancer cells were spiked in the peripheral blood samples (sample A, B and C), and their detection was investigated. KG1a, MCF7 and SK-BR-3 cells were harvest for spiking purpose and concentrated/diluted to a concentration of 1M cells/mL. To demonstrate the existence of specific cancer markers that allow to distinguish its presence in blood, three separated measurements were performed: lysed blood sample, solely cancer cells and cancer spiked blood samples.

For KG1a cells, the cancer cells sample revealed that cell binding occurred to spots of antibodies widely used to characterize peripheral blood cells. Being derived from a macrophage cell population, the antigen similarity

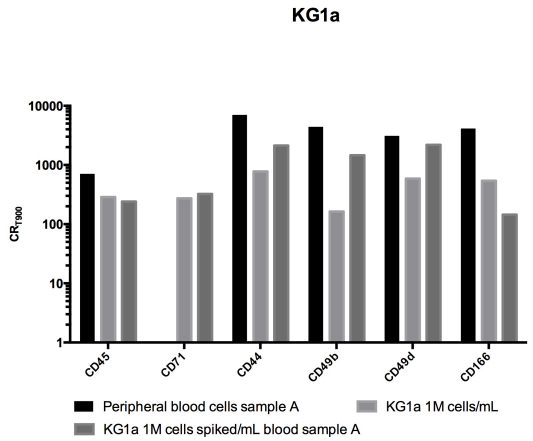

Figure 8. Detection of KG1a cancer cells spiked blood sample A by SPR analysis. Comparison of relevant markers for this cell lineage.

with leukocytes would be expected. Considering all the markers with cell binding curves for both single cells sample and spiked sample, anti-CD71 seems to appear only when KG1a cells are present (see **Figure 8**).

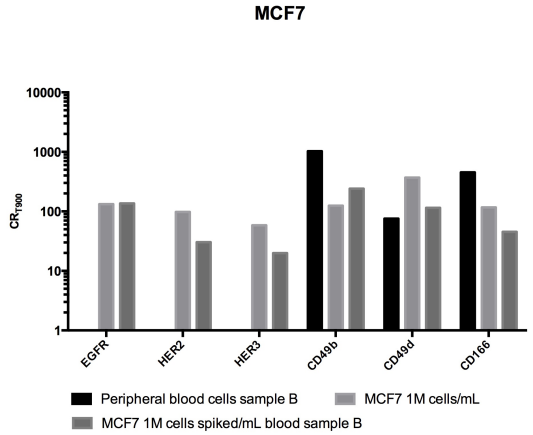

Figure 9. Detection of MCF7 cancer cells spiked blood sample B by SPR analysis. Comparison of relevant markers for this cell lineage.

MCF7 cells show a more distinct antigen profile when comparing cancer cells sample measurement with the peripheral blood sample B (see **Figure 9**). Looking for markers that show cell binding only in the presence of MCF7 cells, three spots are discovered anti-EGFR, anti-HER2 and anti-HER3.

In the same way, SK-BR-3 cells present an antigen profile closer to MCF7 cells than to the peripheral blood sample C (see **Figure 10**). Comparing SK-BR-3 binding spots to the spiked sample a total of five specific SK-BR-3 markers are encountered anti-CD49c, anti-CD71, anti-EpCAM, anti-EGFR, anti-HER2 and anti-HER3.

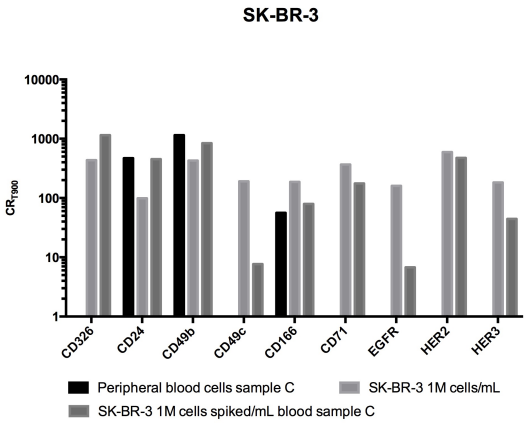

Figure 10. Detection of SK-BR-3 cancer cells spiked blood sample C by SPR analysis. Comparison of relevant markers for this cell lineage.

3.3 Flow cytometry analysis

To validate the detection of cell binding in SPR measurements, antigen quantification was performed by flow cytometry analysis. Regarding SPR analysis, cells from the same cell population used for the cytometry analysis, were measured on a multiplex sensor, ensuring that cell binding signals can be directly compared with the number of antigens determined by cytometry.

In **Figure 11** a scatter plot of all the ABC number and their correspondent CRT_{900} values was constructed. Additionally to this data, two reference limits were imposed: the average ABC value found for the unstained controls in flow cytometry analysis and the average CRT_{900} value from which cell binding becomes visible in the sensor image.

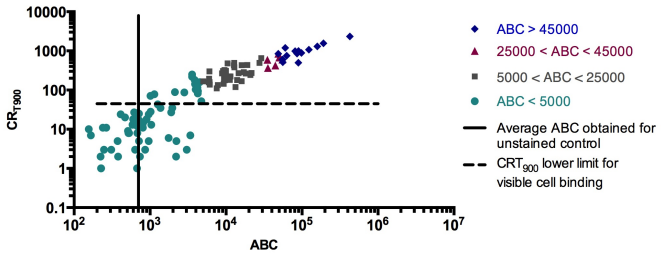

Figure 11. Scatter plot of the ABC value versus CRT_{900} for 36 markers studied for KG1a, MCF7, MG-63, NCI-H460 and SK-BR-3 cells. Data points were distributed into four ABC categories. Horizontal and vertical axis are represented in logarithmic scale to highlight the data distribution. The black and dashed lines represent the average limits of positive detection for both FACS and SPR measurements.

Figure 11 shows a clear positive slope trend between ABC and CRT_{900} values and the distribution of the four ABC groups seems to follow an ascending order. It should also be noted that a logarithmic scale was used, in order to highlight the data distribution.

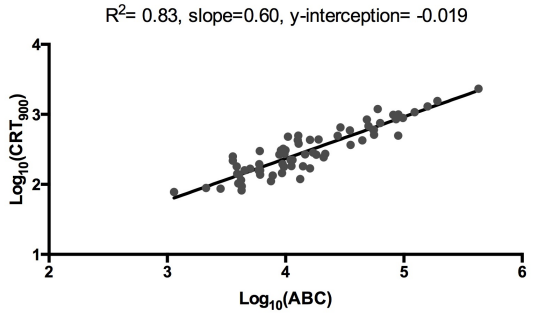

Figure 12. Scatter plot of the ABC value versus CRT_{900} for the data points above cell detection lower limit. At the top of the plot, the linear regression coefficients are shown.

Moreover, the data enclosed in the defined FACS and SPR limits looks to have a linear proportionality. To explore the possibility of a linear regression being present between the two variables under study, the logarithmic (base 10) values of this selected data were calculated and plotted in **Figure 12**. The linear regression fit represented in the plot has a slope of 0.60 and intercepts the y-axis at -0.019. The goodness of the fit has a R^2 value of 0.83. Translating the linear relation to ABC and CRT_{900} absolute values, the expression is presented in **Equation 3**.

$$\log_{10}(\text{CRT}_{900}) = 0.60\log_{10}(\text{ABC}) - 0.019 \qquad (3)$$

Overall, the linear relation found for the logarithmic values of ABC and CRT_{900} indicates that antigen quantification based on SPR intensity can be achieved, even considering that SPR is only sensitive to part of the cell surface. Further testing of SPR technique with more cell lines and calibrated antibody coated beads can provide additional evidence for this relation.

3.4 Image analysis

Up to this point, the analysis of SPR and cytometry results allowed to conclude that spot density and antigen expression influence somehow the cell binding to the sensor spots.

Cell number analysis

The first imaging feature to be analyzed was the number of cells visible on the sensor spots and its relation with the SPR signal intensity. To achieve a gradient of the number of cells biding to the spots, six serial dilutions starting from 1 M cells/mL down to 31 000 cells/mL, were prepared.

The outcome of cell counting revealed that there is a significant CRT_{900} value difference between the highest expressed marker CD49b and the two less expressed markers HER2 and CD71 for the three densities.

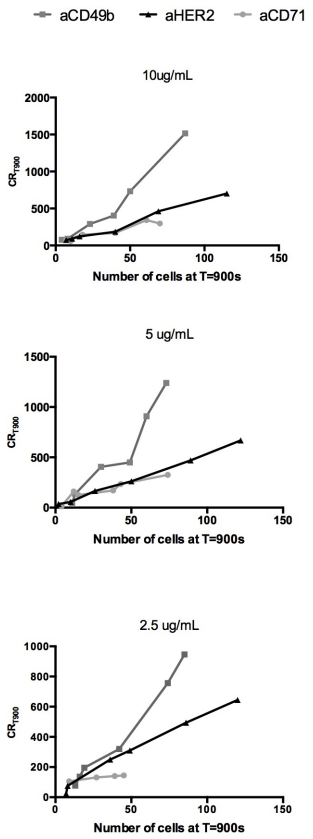

Figure 13. Cell counting analysis. For each of the three tested spot densities (10,5 and 2.5µg/mL) MCF7 cells were counted at 900s of association phase, for anti-CD71, anti-HER2 and anti-CD49b markers.

Here, linear regressions were applied to each marker and spot density as shown in **Table 4**. Analyzing the curve slopes, it seems that, for the same marker, there is no significant difference between spots densities, meaning that the relation between the number of cells and CRT_{900} is not affected by spot density. Additionally, the maximum number of cells for each marker does not show a considerable difference considering the three tested densities. This suggests that spot density does not influence the number of cells landing on a spot.

Table 4. Linear regression coefficients obtained for the relation between cell number and correspondent CRT_{900} values, obtained for three different expressed markers anti-CD71, anti-HER2 and anti-CD49b in three different spot densities 10, 5 and 2.5µg/mL.

Linear regression coefficients									
	anti-CD71			anti-HER2			anti-CD49b		
	R^2	Slope	y-interception	R^2	Slope	y-interception	R^2	Slope	y-interception
10 µg/mL	0.90	4.1	40.56	0.98	5.97	16.41	0.96	17.28	-89.33
5 µg/mL	0.85	3.71	56.70	0.99	5.25	14.69	0.92	17.35	-151.50
2.5 µg/mL	0.87	1.096	97.75	0.99	5.31	28.47	0.98	11.35	-65.93

Regarding the antigen expression, the highest calculated slope corresponds to the highest expressed marker, CD49b, suggesting that for the same number of cells a higher CRT_{900} value is achieved for higher expressed marker. This information comes accordingly to the relation found between the number of the antigens and CRT_{900} value **Figure 12**.

Cell area analysis

The second feature to be studied in this image analysis section was the cell area, and its effect on SPR cell response. The SPR platform IBIS MX96 used throughout this work, has an image resolution of 2 megapixels, where pixel has a size of 5.5 x 5.5 µm. Although being sufficient to identify cells, only significant morphological changes can be precisely detected.

For these reasons, SK-BR-3 cells were measured with three different markers, where a significant increase of cell size as been observed. Anti-CD71, anti-HER2, and anti-CD49b spots were printed with a density of 5µg/mL. Taking the cytometry analysis results into account, the expression levels for these three markers were 35 500 for CD71, 158 838 for HER2 and 20 942 for CD49b.

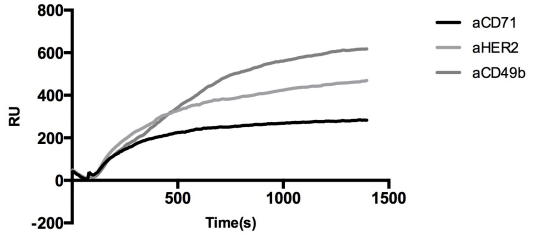

Figure 14. Sensorgrams of SK-BR-3 cells binding to anti-CD71, anti-HER2 and anti-CD49b spots with a density of 5ug/mL. Spots were printed into a G-type sensor with CFM spotter.

In **Figure 14**, sensorgrams for anti-CD71, anti-HER2 and anti-CD49b are presented. Surprisingly, the highest CRT_{900} value does not correspond to highest expressed marker HER2, but to CD49b.

Spot images were selected for the correspondent sensogram curves **Figure 15**. Assuming that cells have an approximate circular shape, five cells were randomly selected and their diameter was measured in pixels. The results for the obtained radius are presented in **Figure 15**. Comparing the radius evolution overtime, is possible to observe that the average radius for cells on anti-CD49b and anti-HER2 spots, increases continuously. For anti-CD71 the average radius shows little variation after time points higher than 300s. Relatively to the absolute average radius value, from 300s of cell association, cells on anti-CD49b spot present the largest radius when compared to anti-HER2 and anti-CD71.

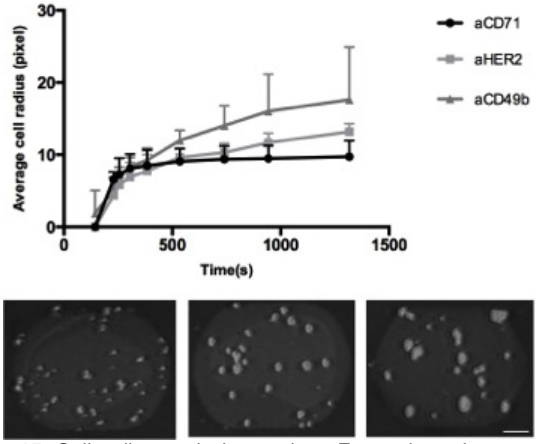

Figure 15. Cell radius analysis overtime. For each marker presented in **Figure 14** five random SK-BR-3 cells were selected and their radius was measured in pixels overtime. Here the average radius is analyzed for nine time points.

Observing the RU curves acquired from the same time points used for image analysis, is possible to distinguish two different characteristic slopes. In the first 500s of cell association a high slope is present, followed by a significantly smaller slope for cell signal over 500s, see **Figure 16**. Taking into account the variations observed for the number of cells and cell radius overtime, one can conclude that the initial high slope is due to a double factor: the increase number of cells landing into the spot and the slight increase of cell radius. The smaller slope observed after the number of cells visible on the spot is constant, seems to be due to the continuous cell spreading.

This observation could open new possibilities to SPR as a biosensor to study the binding behavior of cells to different ligands.

Single cell image analysis

A previous study conducted with the same SPR platform mentioned that small ROIs, per example of cell size, would give rise to higher response with the downside of becoming more sensitive to background noise [13].

Using differential image, a study was conducted to investigate whether a single cell image based measurement was possible.

The sensor background brightness changes accordingly to the scanner angle, therefore a fixed angle of -750m°, corresponding to the background resonance angle, was used. A first image of the sensor was acquired prior to the cell injection, to be continuously subtracted from future images, removing the spot brightness contribution.

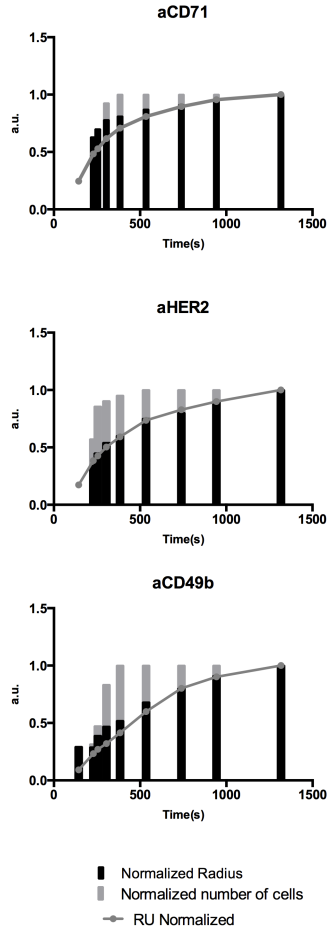

Figure 16. Cell number and radius comparative analysis. SPR sensograms for anti-CD71, anti-HER2 and anti-CD49b **Figure 14** were normalized by the end point RU value. In the same way cell number and radius were normalized by the final value correspondent to the SPR end point value.

For these measurements MCF7 cells were used, and three different spot markers were printed: anti-EpCAM, anti-EGFR and anti-CD24. In **Figure 17** the average cell pixel intensity values obtained for the three single cell areas are shown. From a general point of view, the pixel intensity observed seems to follow a curve similar to a classic SPR RU units sensorgram.

The conducted analysis shows that individual cells can be monitored by the analysis of single cell average pixel intensity. However, the improvement of the imaging hardware with increased resolution and an automatic software for identification of cell positioning is needed and would greatly contribute to the use of SPR as a single cell analyzing technique.

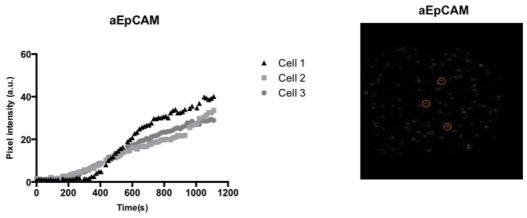

Figure 17. Variation of cell pixel intensity over time. Pixel intensity was analyzed for 3 different cells biding anti-EpCAM spot with a spot density of 10 µg/mL.

4. Conclusion

In this work, the multiplex detection of cancer and peripheral blood cells using Surface Plasmon Resonance Imaging was investigated.

A primary study of the measurement parameters that could affect the cell binding, revealed that the cell signal intensity is proportional to spot antibody density. A maximal response was obtained for antibody densities of 5 and 10ug/mL. A temperature of 37°C and culture medium as measurement buffer, seemed to promote an optimal cell binding.

The 44-plex analysis was conducted on five different cancer cell lines and peripheral blood cells from healthy donors. The obtained results demonstrate that multiplex SPR analysis is capable of characterizing multiple antigens present on the cell surface.

Also, based on the cell binding to specific markers it was possible to identify frequent blood cells such as T-cells and Granulocytes. Additionally, the measurements with spiked blood successfully detected the added cancer cells, proving that a multiplex set up can be used to detect sub-populations in complex samples.

To validate the detection of the cell antigens with SPR, flow cytometry was used to obtain antigen quantification. An interesting relation between antigen expression and the cell SPR signal intensity was discovered. This suggests that SPR cell analysis might be explored as a quantitative detection method for surface antigens.

Further exploring the cell binding detection, an image analysis was conducted to evaluate the contribution of the number of cells and cell area to the SPR signal. As observed in previous studies, a higher number of cells binding to the spot contributes to a higher signal intensity. A new observation was found when comparing different markers expressions of a cell lineage, for the same number of cells a higher signal intensity is achieved for a higher expressed antigen.

Considering the cell area influence, exceptional cases where significant cell spreading occurred, demonstrated

that the signal varies in proportion with the increase of cell radius, independently of antigen expression.

In order to access if an image based single cell SPR analysis could be feasible, a final study was performed on differential sensor images. The pixel intensity variation of a single cell area, indicates that cell binding can be monitored by image processing. Nevertheless, both technological and cell testing efforts should be made to further validate these observations.

In conclusion, the reported results prove that SPR can be considered a viable technique for cell surface antigen characterization and quantification.

References

[1] K. A. Willets and R. P. Van Duyne, "Localized surface plasmon resonance spectroscopy and sensing," *Annual Review of Physical Chemistry*, vol. 58, no. 1, pp. 267–297, 2007, pMID: 17067281. [Online]. Available:

[2] J. Homola, S. S. Yee, and G. Gauglitz, "Surface plasmon resonance sensors: review," *Sensors and Actuators B: Chemical*, vol. 54, no. 1–2, pp. 3 – 15, 1999. [Online]. Available:

[3] A. V. Zayats, I. I. Smolyaninov, and A. A. Maradudin, "Nano-optics of surface plasmon polaritons," *Physics Reports-review Section of Physics Letters*, vol. 408, pp. 131–314, 2005.

[4] *Handbook of Surface Plasmon Resonance*. RCSPublishing, 2008.

[5] M. Couture, S. S. Zhao, and J.-F. Masson, "Modern surface plasmon resonance for bioanalytics and biophysics," *Phys. Chem. Chem. Phys.*, vol. 15, pp. 11 190–11 216, 2013. [Online]. Available:

[6] J. Homola, "Surface plasmon resonance sensors for detection of chemical and biological species," *Chemical Reviews*, vol. 108, no. 2, pp. 462–493, 2008, pMID: 18229953. [Online]. Available:

[7] P. N. Abadian, C. P. Kelley, and E. D. Goluch, "Cellular analysis and detection using surface plasmon resonance techniques," *Analytical Chemistry*, vol. 86, no. 6, pp. 2799–2812, 2014, pMID: 24502446. [Online]. Available:

[8] S. CortÃšs, C. L. Villiers, P. Colpo, R. Couderc, C. Brakha, F. Rossi, P. N. Marche, and M.-B. Villiers, "Biosensor for direct cell detection, quantification and analysis," *Biosensors and Bioelectronics*, vol. 26, no. 10, pp. 4162 – 4168, 2011. [Online]. Available:

[9] K. Chen, H. Obinata, and T. Izumi, "Detection of g protein-coupled receptor-mediated cellular response involved in cytoskeletal rearrangement using surface plasmon resonance," *Biosensors and Bioelectronics*, vol. 25, no. 7, pp. 1675 – 1680, 2010. [Online]. Available:

[10] H. Zhang, L. Yang, B. Zhou, X. Wang, G. Liu, W. Liu, and P. Wang, "Investigation of biological cellâprotein interactions using {SPR} sensor through laser scanning confocal imagingâsurface plasmon resonance system," *Spectrochimica Acta Part A: Molecular and Biomolecular Spectroscopy*, vol. 121, no. 0, pp. 381 – 386, 2014. [Online]. Available:

[11] Y. Yanase, H. Suzuki, T. Tsutsui, T. Hiragun, Y. Kameyoshi, and M. Hide, "The {SPR} signal in living cells reflects changes other than the area of adhesion and the formation of cell constructions," *Biosensors and Bioelectronics*, vol. 22, no. 6, pp. 1081 – 1086, 2007. [Online]. Available:

[12] M. Hide, T. Tsutsui, H. Sato, T. Nishimura, K. Morimoto, S. Yamamoto, and K. Yoshizato, "Real-time analysis of ligand-induced cell surface and intracellular reactions of living mast cells using a surface plasmon resonance-based biosensor," *Analytical Biochemistry*, vol. 302, no. 1, pp. 28 – 37, 2002. [Online]. Available:

[13] I. Stojanović, R. B. Schasfoort, and L. W. Terstappen, "Analysis of cell surface antigens by surface plasmon resonance imaging," *Biosensors and Bioelectronics*, vol. 52, no. 0, pp. 36 – 43, 2014. [Online]. Available:

[14] T. Hiragun, Y. Yanase, K. Kose, T. Kawaguchi, K. Uchida, S. Tanaka, and M. Hide, "Surface plasmon resonance-biosensor detects the diversity of responses against epidermal growth factor in various carcinoma cell lines," *Biosensors and Bioelectronics*, vol. 32, no. 1, pp. 202 – 207, 2012. [Online]. Available:

[15] C. L. Sawyers, "The cancer biomarker problem," *Nature*, vol. 452, no. 7187, pp. 548–552, 04 2008. [Online]. Available:

[16] V. Kulasingam and E. P. Diamandis, "Strategies for discovering novel cancer biomarkers through utilization of emerging technologies," *Nat Clin Prac Oncol*, vol. 5, no. 10, pp. 588–599, 10 2008. [Online]. Available:

[17] Z. Altintas, Y. Uludag, Y. Gurbuz, and I. E. Tothill, "Surface plasmon resonance based immunosensor for the detection of the cancer biomarker carcinoembryonic antigen," *Talanta*, vol. 86, no. 0, pp. 377 – 383, 2011. [Online]. Available:

[18] X. Fang, J. Tie, Y. Xie, Q. Li, Q. Zhao, and D. Fan, "Detection of gastric carcinoma-associated antigen mg7-ag in human sera using surface plasmon resonance sensor," *Cancer Epidemiology*, vol. 34, no. 5, pp. 648 – 651, 2010. [Online]. Available:

[19] *Leukocyte and Stromal Cell Molecules: The CD Markers*. Wiley, 2007.

[20] C. A. Smith, G. T. Williams, R. Kingston, E. J. Jenkinson, and J. J. T. Owen, "Antibodies to cd3/t-cell receptor complex induce death by apoptosis in immature t cells in thymic cultures," *Nature*, vol. 337, no. 6203, pp. 181–184, 01 1989. [Online]. Available:

[21] S. M. Kaech, J. T. Tan, E. J. Wherry, B. T. Konieczny, C. D. Surh, and R. Ahmed, "Selective expression of the interleukin 7 receptor identifies effector cd8 t cells that give rise to long-lived memory cells," *Nat Immunol*, vol. 4, no. 12, pp. 1191–1198, 12 2003. [Online]. Available:

[22] J. Banchereau and R. M. Steinman, "Dendritic cells and the control of immunity," *Nature*, vol. 392, no. 6673, pp. 245–252, 03 1998. [Online]. Available:

[23] ——, "Dendritic cells and the control of immunity," *Nature*, vol. 392, no. 6673, pp. 245–252, 03 1998. [Online]. Available:

[24] M. D. Gunn, V. N. Ngo, K. M. Ansel, E. H. Ekland, J. G. Cyster, and L. T. Williams, "A b-cell-homing chemokine made in lymphoid follicles activates burkitt's lymphoma receptor-1," *Nature*, vol. 391, no. 6669, pp. 799–803, 02 1998. [Online]. Available:

[25] S. Funderud, B. Erikstein, H. C. Ãsheim, K. Nustad, T. Stokke, H. K. Blomhoff, H. Holte, and E. B. Smeland, "Functional properties of cd19 b lymphocytes positively selected from buffy coats by immunomagnetic separation," *European Journal of Immunology*, vol. 20, no. 1, pp. 201–206, 1990. [Online]. Available:

[26] F. Montalvao, Z. Garcia, S. Celli, B. Breart, J. Deguine, N. V. Rooijen, and P. Bousso, "The mechanism of anti-cd20âmediated b cell depletion revealed by intravital imaging," *The Journal of Clinical Investigation*, vol. 123, no. 12, pp. 5098–5103, 12 2013. [Online]. Available:

[27] D. A. A. Vignali, L. W. Collison, and C. J. Workman, "How regulatory t cells work," *Nat Rev Immunol*, vol. 8, no. 7, pp. 523–532, 07 2008. [Online]. Available:

[28] F. Lajaunias, J.-M. Dayer, and C. Chizzolini, "Constitutive repressor activity of cd33 on human monocytes requires sialic acid recognition and phosphoinositide 3-kinase-mediated intracellular signaling," *European Journal of Immunology*, vol. 35, no. 1, pp. 243–251, 2005. [Online]. Available:

[29] T. Schmidt, J. Zündorf, T. Grüger, K. Brandenburg, A.-L. Reiners, J. Zinserling, and N. Schnitzler, "Cd66b overexpression and homotypic aggregation of human peripheral blood neutrophils after activation by a gram-positive stimulus," *Journal of Leukocyte Biology*, vol. 91, no. 5, pp. 791–802, 2012. [Online]. Available:

[30] E. Fonsatti, M. Altomonte, M. R. Nicotra, P. G. Natali, and M. Maio, "Endoglin (cd105): a powerful therapeutic target on tumor-associated angiogenetic blood vessels," *Oncogene*, vol. 22, no. 42, pp. 6557–6563, print 0000. [Online]. Available:

[31] J. Shi, K. Ikeda, Y. Maeda, K. Shinagawa, A. Ohtsuka, H. Yamamura, and M. Tanimoto, "Identification of cd123+ myeloid dendritic cells as an early-stage immature subset with strong tumoristatic potential," *Cancer Letters*, vol. 270, no. 1, pp. 19–29, 2014/11/13. [Online]. Available:

[32] T. Yamashita, J. Ji, A. Budhu, M. Forgues, W. Yang, H. Wang, H. Jia, Q. Ye, L. Qin, E. Wauthier, L. M. Reid, H. Minato, M. Honda, S. Kaneko, Z. Tang, and X. W. Wang, "Epcam-positive hepatocellular carcinoma cells are tumor-initiating cells with stem/progenitor cell features," *Gastroenterology*, vol. 136, no. 3, pp. 1012 – 1024.e4, 2009. [Online]. Available:

[33] H. Habashy, D. Powe, C. Staka, E. Rakha, G. Ball, A. Green, M. Aleskandarany, E. Paish, R. Douglas Macmillan, R. Nicholson, I. Ellis, and J. Gee, "Transferrin receptor (cd71) is a marker of poor prognosis in breast cancer and can predict response to tamoxifen," *Breast Cancer Research and Treatment*, vol. 119, no. 2, pp. 283–293, 2010. [Online]. Available:

[34] T. M. Allen, "Ligand-targeted therapeutics in anticancer therapy," *Nat Rev Cancer*, vol. 2, no. 10, pp. 750–763, 10 2002. [Online]. Available:

[35] Q. Liu, M. Wang, Y. Hu, H. Xing, X. Chen, Y. Zhang, and P. Zhu, "Significance of cd71 expression by flow cytometry in diagnosis of acute leukemia," *Leukemia amp; Lymphoma*, vol. 55, no. 4, pp. 892–898, 2014, pMID: 23962073.

[36] A. Potti, N. Moazzam, K. Ramar, D. S. Hanekom, S. Kargas, and M. Koch, "Cd117 (c-kit) overexpression in patients with extensive-stage small-cell lung carcinoma," *Annals of Oncology*, vol. 14, no. 6, pp. 894–897, 2003.

[37] A. Agaimy, P. H. Wünsch, F. Hofstaedter, H. Blaszyk, P. Rümmele, A. Gaumann, W. Dietmaier, and A. Hartmann, "Minute gastric sclerosing stromal tumors (gist tumorlets) are common in adults and frequently show c-kit mutations," *The American Journal of Surgical Pathology*, vol. 31, no. 1, 2007.

[38] J. P. Murphy and D. M. Pinto, "Temporal proteomic analysis of igf-1r signalling in mcf-7 breast adenocarcinoma cells," *PROTEOMICS*, vol. 10, no. 9, pp. 1847–1860, 2010. [Online]. Available:

[39] E. Rozengurt, J. Sinnett-Smith, and K. Kisfalvi, "Crosstalk between insulin/insulin-like growth factor-1 receptors and g protein-coupled receptor signaling systems: A novel target for the antidiabetic drug metformin in pancreatic cancer," *Clinical Cancer Research*, vol. 16, no. 9, pp. 2505–2511, 2010.

[40] J. Taylor-Papadimitriou, J. Burchell, D. Miles, and M. Dalziel, "Muc1 and cancer," *Biochimica et Biophysica Acta (BBA) - Molecular Basis of Disease*, vol. 1455, no. 2003, pp. 301 – 313, 1999. [Online]. Available:

[41] P. Mukherjee, L. Pathangey, J. Bradley, T. Tinder, G. Basu, E. Akporiaye, and S. Gendler, "Muc1-specific immune therapy generates a strong anti-tumor response in a muc1-tolerant colon cancer model," *Vaccine*, vol. 25, no. 9, pp. 1607 – 1618, 2007. [Online]. Available:

[42] L. A. Snyder, T. J. Goletz, G. R. Gunn, F. F. Shi, M. C. Harris, K. Cochlin, C. McCauley, S. G. McCarthy, P. J. Branigan, and D. M. Knight, "A muc1/il-18 {DNA} vaccine induces anti-tumor immunity and increased survival in {MUC1} transgenic mice," *Vaccine*, vol. 24, no. 16, pp. 3340 – 3352, 2006. [Online]. Available:

[43] B. M. Kurbanov, C. C. Geilen, L. F. Fecker, C. E. Orfanos, and J. Eberle, "Efficient trail-r1/dr4-mediated apoptosis in melanoma cells by tumor necrosis factor-related apoptosis-inducing ligand (trail)," *J Investig Dermatol*, vol. 125, no. 5, pp. 1010–1019, 10 2005. [Online]. Available:

[44] H. Vincent, P.-P. Claire, T. Marion, D. Ludovic, J. Bernard, P. Jean-Jacques, and G. Thierry, "Sensitivity of prostate cells to trail-induced apoptosis increases with tumor progression: Dr5 and caspase 8 are key players," *The Prostate*, vol. 66, no. 9, pp. 987–995, 2006. [Online]. Available:

[45] K. Shibuya, R. Komaki, T. Shintani, S. Itasaka, A. Ryan, J. M. Jürgensmeier, L. Milas, K. Ang, R. S. Herbst, and M. S. O'Reilly, "Targeted therapy against vegfr and egfr with zd6474 enhances the therapeutic efficacy of irradiation in an orthotopic model of human non–small-cell lung cancer," *International Journal of Radiation Oncology *Biology *Physics*, vol. 69, no. 5, pp. 1534–1543, 2014/11/13. [Online]. Available:

[46] G. Klement, S. Baruchel, J. Rak, S. Man, K. Clark, D. J. Hicklin, P. Bohlen, and R. S. Kerbel, "Continuous low-dose therapy with vinblastine and vegf receptor-2 antibody induces sustained tumor regression without overt toxicity," *The Journal of Clinical*

Investigation, vol. 105, no. 8, pp. R15–R24, 4 2000. [Online]. Available:

[47] R. Sordella, D. W. Bell, D. A. Haber, and J. Settleman, "Gefitinib-sensitizing egfr mutations in lung cancer activate anti-apoptotic pathways," *Science*, vol. 305, no. 5687, pp. 1163–1167, 2004. [Online]. Available:

[48] N. Normanno, A. D. Luca, C. Bianco, L. Strizzi, M. Mancino, M. R. Maiello, A. Carotenuto, G. D. Feo, F. Caponigro, and D. S. Salomon, "Epidermal growth factor receptor (egfr) signaling in cancer," *Gene*, vol. 366, no. 1, pp. 2 – 16, 2006. [Online]. Available:

[49] B. R. Voldborg, L. Damstrup, M. Spang-Thomsen, and H. S. Poulsen, "Epidermal growth factor receptor (egfr) and egfr mutations, function and possible role in clinical trials," *Annals of Oncology*, vol. 8, no. 12, pp. 1197–1206, 1997. [Online]. Available:

[50] J. Mendelsohn and J. Baselga, "The egf receptor family as targets for cancer therapy," *Oncogene*, vol. 19, no. 56, p. 6550â6565, December 2000. [Online]. Available:

[51] D. Harari and Y. Yarden, "Molecular mechanisms underlying erbb2/her2 action in breast cancer," *Oncogene*, vol. 19, no. 53, December 2000. [Online]. Available:

[52] R. Nahta, D. Yu, M.-C. Hung, G. N. Hortobagyi, and F. J. Esteva, "Mechanisms of disease: understanding resistance to her2-targeted therapy in human breast cancer," *Nat Clin Prac Oncol*, vol. 3, no. 5, pp. 269–280, 05 2006. [Online]. Available:

[53] N. V. Sergina, M. Rausch, D. Wang, J. Blair, B. Hann, K. M. Shokat, and M. M. Moasser, "Escape from her-family tyrosine kinase inhibitor therapy by the kinase-inactive her3," *Nature*, vol. 445, no. 7126, pp. 437–441, 01 2007. [Online]. Available:

[54] M. E. B. J. S. K. D. C. D. E. P. C. A. P. G. H. D. M. Kristiansen G, Winzer KJ, "Cd24 expression is a new prognostic marker in breast cancer." *Clinical Cancer Reasearch*, vol. 9, 2003.

[55] S. Aigner, Z. M. Sthoeger, M. Fogel, E. Weber, J. Zarn, M. Ruppert, Y. Zeller, D. Vestweber, R. Stahel, M. Sammar, and P. Altevogt, "Cd24, a mucin-type glycoprotein, is a ligand for p-selectin on human tumor cells," *Blood*, vol. 89, no. 9, pp. 3385–3395, 1997.

[56] K. Polyak and R. A. Weinberg, "Transitions between epithelial and mesenchymal states: acquisition of malignant and stem cell traits," *Nat Rev Cancer*, vol. 9, no. 4, pp. 265–273, 04 2009. [Online]. Available:

[57] B. Mayer, K. Jauch, F. Schildberg, I. Funke, U. GÃŒnthert, C. Figdor, and J. Johnson, "De-novo expression of {CD44} and survival in gastric cancer," *The Lancet*, vol. 342, no. 8878, pp. 1019 – 1022, 1993, originally published as Volume 2, Issue 8878. [Online]. Available:

[58] M. Zöller, "Cd44: can a cancer-initiating cell profit from an abundantly expressed molecule?" *Nat Rev Cancer*, vol. 11, no. 4, pp. 254–267, 04 2011. [Online]. Available:

[59] R. L. Brown, L. M. Reinke, M. S. Damerow, D. Perez, L. A. Chodosh, J. Yang, and C. Cheng, "Cd44 splice isoform switching in human and mouse epithelium is essential for epithelial-mesenchymal transition and breast cancer progression," *The Journal of Clinical Investigation*, vol. 121, no. 3, pp. 1064–1074, 3 2011. [Online]. Available:

[60] S. Yachida and C. A. Iacobuzio-Donahue, "The pathology and genetics of metastatic pancreatic cancer," *Archives of Pathology & Laboratory Medicine*, vol. 133, no. 3, pp. 413–422, 2014/11/13 2009. [Online]. Available:

[61] W. Guo and F. G. Giancotti, "Integrin signalling during tumour progression," *Nat Rev Mol Cell Biol*, vol. 5, no. 10, pp. 816–826, 10 2004. [Online]. Available:

[62] R. Hosotani, M. Kawaguchi, T. Masui, T. Koshiba, J. Ida, K. Fujimoto, M. Wada, R. Doi, and M. Imamura, "Expression of integrin alphavbeta3 in pancreatic carcinoma: Relation to mmp-2 activation and lymph node metastasis," *Pancreas*, vol. 25, no. 2, 2002.

[63] K. Okazaki, Y. Nakayama, K. Shibao, K. Hirata, N. Nagata, and H. Itoh, "Enhancement of metastatic activity of colon cancer as influenced by expression of cell surface antigens," *Journal of Surgical Research*, vol. 78, no. 1, pp. 78 – 84, 1998. [Online]. Available:

[64] G. C. Tucker, "Alpha v integrin inhibitors and cancer therapy," *Current opinion in investigational drugs (London, England : 2000)*, vol. 4, no. 6, June 2003. [Online]. Available:

[65] P. Dalerba, S. J. Dylla, I.-K. Park, R. Liu, X. Wang, R. W. Cho, T. Hoey, A. Gurney, E. H. Huang, D. M. Simeone, A. A. Shelton, G. Parmiani, C. Castelli, and M. F. Clarke, "Phenotypic characterization of human colorectal cancer stem cells," *Proceedings of the National Academy of Sciences*, vol. 104, no. 24, pp. 10 158–10 163, 2007. [Online]. Available:

[66] A. S. Goldstein, J. Huang, C. Guo, I. P. Garraway, and O. N. Witte, "Identification of a cell of origin for human prostate cancer," *Science*, vol. 329, no. 5991, pp. 568–571, 2010. [Online]. Available:

[67] P. W. R. J. d. J. R. Webb, K. Milne and B. H. Nelson, "Tumor-infiltrating lymphocytes expressing the tissue resident memory marker cd103 are associated with increased survival in high-grade serous ovarian cancer," *Clinical Cancer Research*, vol. 20, 2014.

[68] K. D. Sutherland and A. Berns, "Cell of origin of lung cancer," *Molecular Oncology*, vol. 4, no. 5, pp. 397 – 403, 2010, thematic Issue: Stem Cells and Cancer. [Online]. Available:

[69] C. A. Maurer, H. Friess, B. Kretschmann, S. Wildi, C. MÃŒller, H. Graber, M. Schilling, and M. W. BÃŒchler, "Over-expression of icam-1, vcam-1 and elam-1 might influence tumor progression in colorectal cancer," *International Journal of Cancer*, vol. 79, no. 1, pp. 76–81, 1998. [Online]. Available:

[70] S. P. Perfetto, P. K. Chattopadhyay, and M. Roederer, "Seventeen-colour flow cytometry: unravelling the immune system," *Nat Rev Immunol*, vol. 4, no. 8, pp. 648–655, 08 2004. [Online]. Available:

[71] N. Robillard, M. C. Bene, P. Moreau, and S. Wuilleme, "A single-tube multiparameter seven-colour flow cytometry strategy for the detection of malignant plasma cells in multiple myeloma," *Blood Cancer Journal*, vol. 3, pp. e134–, 08 2013. [Online]. Available:

[72] A. TÃ¡rnok and A. O. Gerstner, “Clinical applications of laser scanning cytometry,” *Cytometry*, vol. 50, no. 3, pp. 133–143, 2002. [Online]. Available:

[73] R. B. Schasfoort, A. E. Bentlage, I. Stojanovic, A. van der Kooi, E. van der Schoot, L. W. Terstappen, and G. Vidarsson, “Label-free cell profiling,” *Analytical Biochemistry*, vol. 439, no. 1, pp. 4 – 6, 2013. [Online]. Available: